Atmos. Chem. Phys., 24, 1627–1639, 2024
https://doi.org/10.5194/acp-24-1627-2024

Atmospheric Chemistry and Physics
Open Access
EGU

Evolution of nucleophilic high molecular-weight organic compounds in ambient aerosols: a case study

Chen He[1], Hanxiong Che[2], Zier Bao[2], Yiliang Liu[2], Qing Li[2], Miao Hu[3], Jiawei Zhou[2], Shumin Zhang[4], Xiaojiang Yao[2], Quan Shi[1], Chunmao Chen[1], Yan Han[2], Lingshuo Meng[2], Xin Long[2], Fumo Yang[5], and Yang Chen[2]

[1]State Key Laboratory of Heavy Oil Processing, China University of Petroleum, Beijing 102249, China
[2]Research Center for Atmospheric Environment, Chongqing Institute of Green and Intelligent Technology, Chinese Academy of Sciences, Chongqing 400714, China
[3]CNOOC Institute of Chemicals & Advanced Materials, Beijing 102200, China
[4]Institute of Basic Medicine and Forensic Medicine, North Sichuan Medical College, Nanchong 637000, Sichuan, China
[5]Department of Environmental Science and Engineering, College of Architecture and Environment, Sichuan University, Chengdu 610065, China

Correspondence: Yang Chen (chenyang@cigit.ac.cn)

Received: 8 May 2023 – Discussion started: 6 June 2023
Revised: 28 November 2023 – Accepted: 16 December 2023 – Published: 6 February 2024

Abstract. Nucleophilic high molecular-weight organic compounds (HMWOCs) are sensitive to protons (H^+) in Fourier transform ion cyclotron resonance mass spectrometry (FT-ICR MS) analysis. A comprehensive evaluation of the diurnal evolution of nucleophilic HMWOCs was performed. HMWOCs aged significantly in daily cycles, accompanied by functionality shifts, particularly oxygenated and reduced nitrogen (CHON and CHN) as well as oxygenated organics. The intensities of high molecular-weight (HMW) oxygenated compounds increased during both daytime and nighttime. The daytime evolution produced more nitrogen-containing compounds with carboxylic group (–COOH) homologues with molecular weights greater than 300, while the nighttime evolution produced mostly small CHON compounds (molecular weights < 300). During evolution, nighttime CHON removals were observed; meanwhile, carboxylation was also identified in CHON groups. The daytime evolution produced significantly more reduced-nitrogen-containing compounds; a day- and nighttime increase in CHN compounds with five members was also observed. This study can provide insights into the aging of less polar organic aerosols.

1 Introduction

Organic aerosol (OA) is a key component of atmospheric aerosols, accounting for up to 90 % of submicron aerosols (Zhang et al., 2015; Tao et al., 2017; Zhang et al., 2007). OA affects solar radiation forcing, fog-cloud process, and human health (Pöschl, 2005; Creamean et al., 2014). The condensation of semivolatile vapors that are more oxidized onto primary OA can lead to the evolution of OA during their atmospheric lives (Jimenez et al., 2009), and the evolution can also be caused by heterogeneous processes in the aerosol phase (Ervens et al., 2011).

OAs can undergo evolution during their lifetimes, resulting in changes in physicochemical properties (Ditto et al., 2021). The aged biomass-burning-emitted aerosols can be important sources of brown carbon (BrC) (Hodshire et al., 2019). During evolution, important components of humic-like substances (HULIS), such as organosulfate and organonitrates, have been identified and observed in both laboratory and field measurements (Hallquist et al., 2009; Liggio and Li, 2006; K. Li et al., 2017; Liu et al., 2015). The heterogeneous reactions, such as acid–base reactions of amines and ammonia with organic acids and carbonyls, can gener-

ate nitrogen- and oxygen-containing organics (Ervens et al., 2011; Zhang et al., 2015; George et al., 2015). The reduced-nitrogen-containing compounds can be from the reactions of amines and ammonia and carbonyls (Zarzana et al., 2012; Liu et al., 2015). These processes were important during long-range transport and severe haze formation due to stagnant air conditions in China (H. Li et al., 2017).

The evolution of high molecular-weight organic compounds (HMWOCs, molecular weight (M.W.) larger than 200) is still an unsolved issue. For example, the overall oxidative state was commonly observed to increase, but it was not observed how the oxidation and other processing occurred in HMWOCs. Most recently, online aerosol mass spectrometry has been widely used in evaluating OA, but the loss of molecular information resulted in difficulties in investigating the aerosol HMWOCs (Zhang et al., 2011; Ditto et al., 2018). HMWOCs, commonly containing elements such as C, H, O, N, and S, can reach up to 1000 Da in M.W. (Ervens et al., 2011). As they are class of potentially light-absorbing components and precipitation participants, it is vital to investigate the environmental behavior of HMWOCs to fully understand the impact of OA (Yun et al., 2019; Bandowe and Meusel, 2017).

Fourier transform ion cyclotron resonance mass spectrometry (FT-ICR MS) is capable of extremely high mass accuracy and resolution for chemical analysis. It has been utilized extensively for characterizing complex organic mixtures of atmospheric OA (Xie et al., 2020; Jiang et al., 2014; Bianco et al., 2018). The method has been used to study HUMIC-like substances, typically biomass burning and coal combustion aerosols (Li et al., 2022; Song et al., 2022; Tang et al., 2020; Laskin et al., 2014; Wang et al., 2019). FT-ICR MS has been widely used in water-soluble organic carbon (WSOC) research using the negative-ion (–) electrospray ionization (ESI) mode. The (–)ESI mode has a good response on components in WSOC with functional groups of –OH and –COOH (Li et al., 2022; Zhang et al., 2021; He et al., 2022). Until recently, high molecular-weight (HMW) hydrophobic organic species, such as ester, hydrocarbons (C_xH_y), fatty acid, and reduced-nitrogen-containing compounds, were understood in only a limited way in ambient particulate matter (PM) samples. CHN and CHON compounds are favorably detected in positive-ion ESI ((+)ESI) mode compared to (–)ESI mode (Lin et al., 2012). This study will investigate the processing of HMW carbonyls, esters, amines, and other nitrogen-containing functional groups since they can form $[M+H]^+$ ions in electrospray ionization operation positive-ion mode (Kanawati et al., 2008; C. He et al., 2021).

We present the molecular description of the diurnal evolution of HMWOCs that is sensitive to the (+)ESI mode in FT-ICR MS analysis to explore a wider context of HMWOCs. In this study, ambient $PM_{2.5}$ samples were collected for 5.5 h for four samples according to a daily cycle, labeled as morning, afternoon, and night as well as midnight and early morning (MEM) in an urban area in East China during spring for OA aging analysis. As a typical metropolitan area in China, the sampling location is influenced by local coal burning, biomass burning, traffic, and residual emissions as well as long-range transport. The molecular-level characterization of HMWOCs was explored, and organic subgroups' chemical composition and evolution under real-world conditions were identified. This study can expand the understanding of HMWOCs' evolution in daily cycles and support the evaluation of the impact of organic aerosols.

2 Materials and methods

2.1 Sample collection

The sampling site was located on the rooftop of a commercial building (33.6047° N, 119.0734° E) with a height of 45 m above the ground. The site is in a typical urban environment in Huanan, East China, with roads, parks, and residential areas nearby. Emissions from restaurants, biomass, and coal burning from villages influence the region.

A high-volume sampler (Thermo Inc., USA) was used for $PM_{2.5}$ sampling at a flow rate of 1.13 $m^3\,min^{-1}$. $PM_{2.5}$ was collected using a quartz filter (Whatman Inc. USA). The filter was pre-baked using a Muffle furnace at 600 °C to diminish organic species. Sampling periods are at midnight and in the early morning (MEM) (23:00–04:30), in the morning (05:00–10:30), in the afternoon (11:00–16:30), and at night (17:00–22:30). A total of 52 samples was collected to describe the pattern of $PM_{2.5}$ chemical composition, and samples from 20 to 21 April 2021 were selected for FT-ICR MS analysis.

The routine $PM_{2.5}$ chemical composition was analyzed, including carbonaceous species, water-soluble ions (SO_4^-, NO_3^-, NH_4^+, Cl^-, and Na^+), and elemental species. The protocols of these analyses are available in the literature and the Supplement to this paper (Wang et al., 2018). The samples were punched from the quartz filter with an area of 0.526 cm^2. Then, the samples from the same collection time were immersed using 10 mL acetonitrile with sonication for 10 min three times. The acquired acetonitrile (ACN) solutions from the same sampling time were gathered, combined, and concentrated to 1 mL for FT-ICR MS analysis.

2.2 FT-ICR MS analysis

The FT-ICR MS analysis of organic aerosol was carried out on a 7.0 T Bruker Solarix 2XR FT-ICR mass spectrometer. The mixture of acetonitrile extract was vaporized to dry. Then, the dry extract was reconstituted with water, and methanol was added proportionally to the water solution before FT-ICR MS analysis. The samples were dissolved in methanol at a concentration of about 50 mg L for the ESI analysis. The samples were injected into the ionization source at 120 $\mu L\,h^{-1}$ through a syringe pump. The typical operating conditions for positive-ion ESI analysis were

as follows: a capillary voltage of −4.0 kV and a capillary exit voltage of 200 V. Ions were accumulated in the hexapole for 0.05 s and were then transferred into the ICR cell with a time-of-flight (ToF) of 0.7 ms. The ion transformation parameter for the quadrupole (Q1) was optimized at m/z 200. The mass range was m/z 150–1000. A total of 128 scans with 4×10^6 data points were accumulated to enhance the signal-to-noise ratio. Details of FT-ICR MS calibration and data processing are provided in the Supplement. Briefly, FT-ICR MS was calibrated using a reference list formed by the manually assigned known formula ($^{12}C_{0–100}$, $^{1}H_{0–200}$,$^{14}N_{0–10}$,$^{16}O_{0–20}$, and $^{32}S_{0–2}$) in data analysis.

2.3 FT-ICR MS data-related parameters integration

A modified aromatic index (AI_{mod}) and double-bond equivalent (DBE) were calculated for each assigned formula, according to Koch and Dittmar. (2006). The Kendrick mass defect (KMD) was calculated according to Stenson et al. (2003). The intensity-weighted average of elements (C, H, O, N, S), formulae (CHO, CHON, CHOS, CHONS), and other parameters (H/C, O/C, DBE, KMD, and AI_{mod}) were calculated for each sample. Molecular formulae were further assigned to the following groups as described by Seidel et al. (2014) and Antony et al. (2014).

The OS_c is used to describe the composition of a complex mixture of organics undergoing oxidation processes. The OS_c is calculated for an assignable molecular formulae as (Kroll et al., 2011)

$$OS_c = -\sum_i OS_i \frac{n_i}{n_C}, \quad (1)$$

where OS_i is the oxidation state associated with the element I and n_i/n_C is the molar ratio of element I to carbon within the molecule. Other details of the data analysis are also available in the Supplement.

When calculating OS_c, the two elements, nitrogen and oxygen, were considered. In positive ESI mode, the valence of N was regarded as −3. Also, the S element was not considered because no S-containing molecules were detected in the sample in positive ESI mode.

3 Results and discussion

3.1 Overview of molecular characterization of organic aerosols

The overview of the sampling site is available in the Supplement. The concentration-time profile is shown in Fig. S1 in the Supplement. Among all 52 samples, although the mass concentration of $PM_{2.5}$ showed a fluctuating trend in a range of 32–81 $\mu g\,m^{-3}$, the fraction of organic carbon was stable with a range of 0.18–0.21 (Fig. S1). During the sampling period, wind came from almost all directions, strongly from the north, south, and east and especially the west on a daily basis (Figs. S2 and S3). Moreover, the meteorological parameters were also stable during the sampling. Therefore, we picked one of these days to evaluate the daily evolution of HMWOCs as the representative sample.

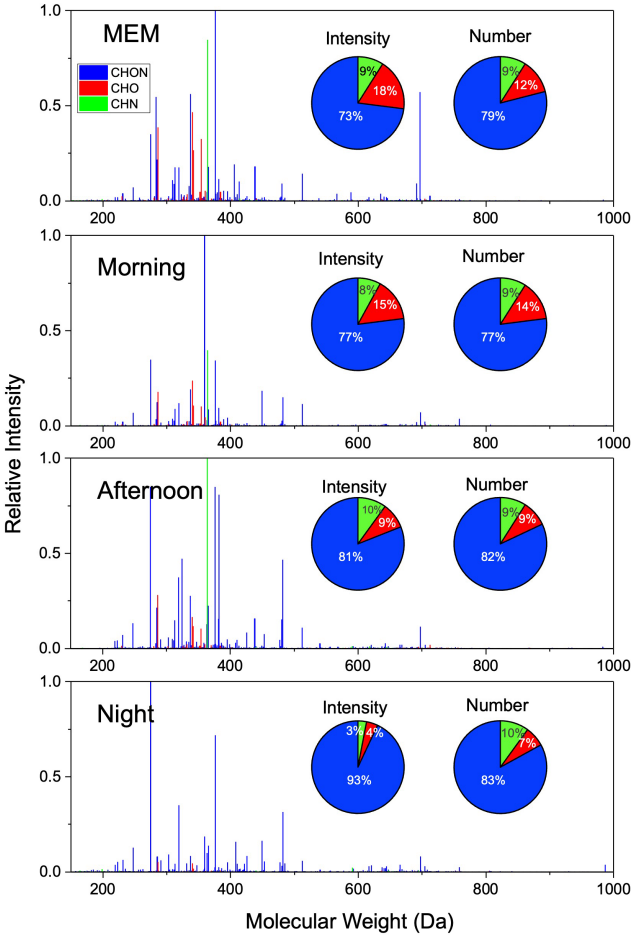

Figure 1. Mass spectra and distribution of relative intensity and formula number of CHON, CHO, and CHN compounds detected by positive-ion ESI FT-ICR MS.

During the observation, the average concentrations of organic carbon (OC) were 12.8 $\mu g\,m^{-3}$, following an order of 12.7 $\mu g\,m^{-3}$ (night), 12.6 $\mu g\,m^{-3}$ (afternoon), 11.1 $\mu g\,m^{-3}$ (morning), and 9.4 $\mu g\,m^{-3}$ (MEM). The concentrations of secondary organic carbon were also estimated as 5.1 $\mu g\,m^{-3}$ (46.0 %), 5.0 $\mu g\,m^{-3}$ (39.3 %), 5.6 $\mu g\,m^{-3}$ (43.8 %), and 4.9 $\mu g\,m^{-3}$ (51.6 %), following the order of night ≈ morning > afternoon > MEM.

A summary of acquired parameters for four samples from FT-ICR MS is shown in Table 1, and the samples are marked with MEM, morning, afternoon, and night. Among four samples, a number of formulas between 5781 and 6566 was detected, with an order of morning < MEM < afternoon < night. The average molecular weights of all four samples were as follows: morning (393 Da) < afternoon (395 Da) < MEM (402 Da) < night

Table 1. Summary of molecular parameters of FT-ICR MS results among four samples during the different periods.

		Number frequency	Molecular weight (Da)	O/C_w	H/C_w	DBE	DBE / C
Midnight and early morning	All	5859	402	0.12	1.69	6.01	0.26
	CHO	715	345	0.13	1.47	6.88	0.31
	CHN	502	385	0	1.3	11.69	0.53
	CHON	4642	418	0.14	1.79	5.08	0.21
Morning	All	5781	393	0.12	1.66	6.35	0.26
	CHO	785	348	0.13	1.48	6.92	0.31
	CHN	531	482	0	1.43	12.23	0.41
	CHON	4465	402	0.13	1.74	5.66	0.23
Afternoon	All	6376	395	0.12	1.75	5.74	0.25
	CHO	606	368	0.13	1.47	7.03	0.31
	CHN	565	385	0	1.29	11.65	0.53
	CHON	5205	399	0.13	1.84	4.84	0.21
Night	All	6566	406	0.13	1.8	5.13	0.21
	CHO	432	429	0.12	1.46	8.22	0.31
	CHN	648	416	0	1.51	9.12	0.37
	CHON	5486	405	0.14	1.82	4.88	0.2

(406 Da). The relative-intensity-weighted element ratios, such as O/C_w and H/C_w, were highest at night, with values of 0.13 and 0.80, respectively, suggesting higher oxidation and saturation levels at night compared to the other three stages. The relative-intensity-weighted carbon-normalized DBE (DBE/C_w) was the lowest at night (0.21), also suggesting a high saturation level of organic compounds, possibly due to primary emissions of OA.

The reconstructed (+)ESI FT-ICR MS measurements of four samples are shown in Fig. 1. Most organic compounds were found M.W. between 200 and 400 Da. All the compounds in the organic aerosol are clustered into oxygenate (CHO) compounds, oxygen- and nitrogen-containing (CHON) compounds, and reduced-nitrogen-containing (CHN) groups. No sulfur-containing compounds were detected in the (+)ESI mode. On an intensity basis, CHON is the largest subgroup, followed by the CHO and CHN subgroups. The CHON group accounted for 73 % of the relative intensity in the MEM and increased to 77 %, 81 %, and 93 % in the morning, in the daytime, and at night. CHN decreased from 10 % to 3 % after sunset. The result implies that daytime photooxidation significantly affected the chemical nature of HMWOCs. In the following results and discussion, a detailed analysis is performed for the nature of daily HMWOC aging.

3.2 Evolution of CHO compounds and functionality

In the (+)ESI mode, the CHO group is favorably detected as carbonyl and ester compounds, but we cannot simply regard those compounds as carbonyl and ester compounds because they are highly likely to contain -COOH or -OH in one molecule. (Ditto et al., 2021). In number frequency, CHO increased from 12 % (MEM) to 14 % (morning) and then decreased to 7 % until the night. CHO molecules contained up to 10 oxygen atoms, but most of the CHO compounds had less than 4 oxygen atoms, i.e., 74.7 % in MEM, 73.5 % in the morning, 69.5 % in the afternoon, and 72.2 % at night.

As shown in Fig. 2, a classification was performed based on the iteration of Antony et al. (2014). We used Van Krevelen diagrams and the criteria from Antony et al. (2014). The classification of saturated hydrocarbons, unsaturated hydrocarbons, lipids, lignin, and polyphenols is only used as a reference for a better understanding of the distribution of organic molecules and the corresponding environmental impacts. The saturated hydrocarbons, including lipids, alkanes, and aliphatics, were dominant, and they were mainly from traffic (Zhang et al., 2011), biogenic emissions, biomass burning (Chen et al., 2014), alcohol synthesis (Ao et al., 2018), and biofuels (Rice et al., 2019). From the point of view of number frequencies, there were 1.2 times more unsaturated hydrocarbons in the MEM sample than in the morning, 1.3 times more in the MEM sample than in the afternoon, and the same amount in the MEM and the night samples. Both samples' frequency was promoted by traffic emissions but removed by daytime photochemical activities (Mcguire et al., 2014).

Figure 3 illustrates the DBE against carbon number with color bars denoting the numbers of oxygen. The CHO compounds showed the highest DBE up to 26. Among them, CHO compounds with less than 4 oxygen atoms, less than 25 carbon atoms, and a DBE between 4 and 16 were favorable phenol compounds with one or two aromatic rings (Yu et al., 2016). However, the HMW CHO group that had ≥ 25 car-

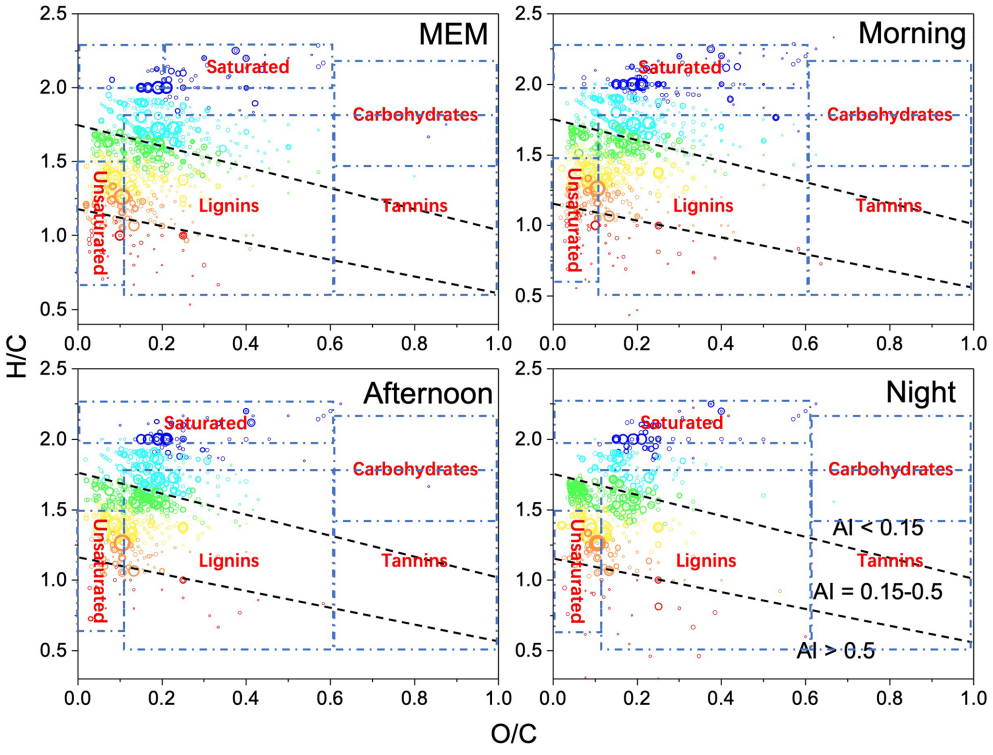

Figure 2. Van Krevelen diagrams (H/C vs. O/C ratio) for CHO species with various aromatic index (AI) value ranges. The dashed lines separate the different AI regions. The size of the symbols reflects the relative peak intensities of molecular formulae on a logarithmic scale.

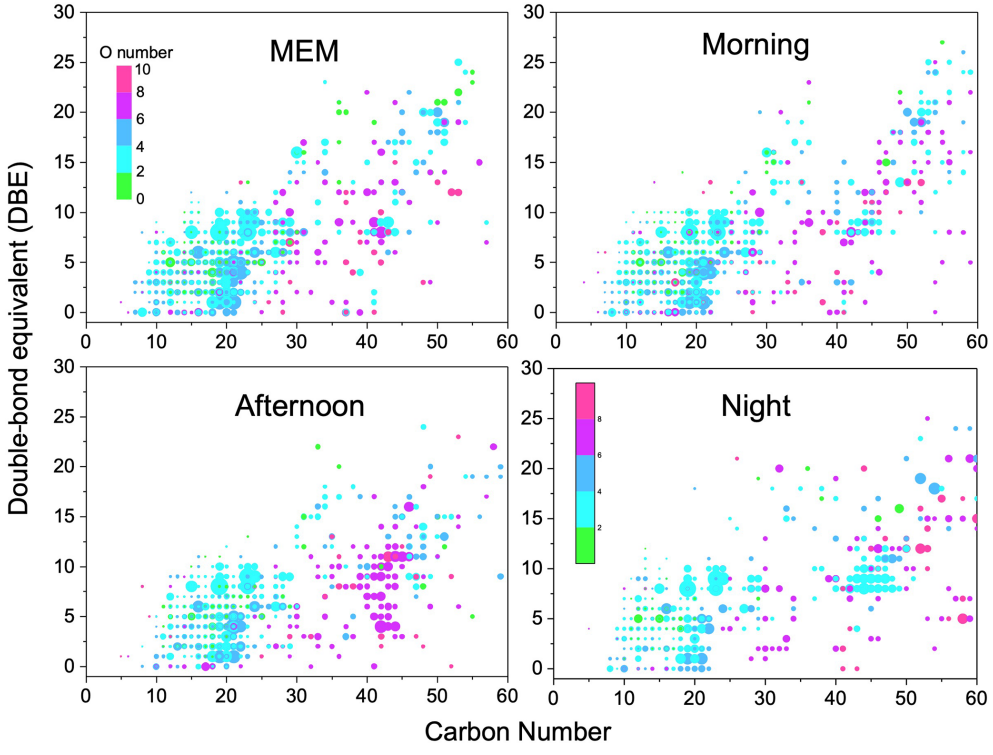

Figure 3. Carbon number vs. double-bond equivalent (DBE) for CHO species. The color bar denotes the number of O atoms. The size of the symbols reflects the relative peak intensities of molecular formulae on a logarithmic scale.

bon atoms commonly had ≥ 6 oxygen atoms. They were recognized as HUMIC-like substances that were abundant with –OH, –COOH, and –CHO but showed an absence of nitrogen (Kurek et al., 2020). Figure S5 in the Supplement implies that the highest carbon oxidation state (OS_c) occurred in compounds with around 15 carbon atoms.

The daytime photochemical activities very strongly change the functionality of CHO compounds. For example, CHO with 20 carbon atoms was observed with more oxygen atoms in the morning and afternoon samples than that in MEM and at night. Particularly, CHO compounds with carbon numbers between 40 and 50 were prominent in the afternoon, possibly due to the formation of –C=O and –COO via daytime photochemical reactions. Then, at night, organic compounds containing more oxygen atoms were found (O number > 6, DBE > 5, and carbon atoms > 50). Meanwhile, a batch of primary OA and less-oxidized secondary organic aerosol (SOA) was also observed, such as CHO compounds with between 45 and 50 carbon atoms, a DBE between 5–10, and between 0 and 2 O atoms. In addition, after serious aging, the highly oxidized CHO compounds with more than eight oxygen atoms significantly increased in the night and MEM samples (Huang et al., 2014).

As shown in Fig. 4, the KMD analysis of CHO compounds was performed. Many homologues of CHO compounds are present as the "core" molecules plus $(CO)_n$ ($n = 0, 1, 2, 3, \ldots$) as a result of carbonyl formation. Among these CHO homologues with KMD_{CO} between 0.4 and 0.0 and less than or equal to four oxygen atoms, carbonyl was favorably resistant or produced in the morning vs. the MEM scenario. However, in the afternoon vs. morning scenario (Fig. 4b) as well as the night vs. afternoon scenario (Fig. 4c), the removal of carbonyls existed among CHO with 1 to 10 oxygen atoms. Likewise, the formation of carboxylic acids (–COOH), represented by $(COO)_n$ homologues, was significant in the morning and removed in both the afternoon and at night, suggesting continuing a destruction of carboxylic acids. Interestingly, the CHO compounds with oxygen numbers less or equal to two continued forming without solar radiation at night. The removal of carbonyls could be attributed to further oxidation to carboxylic acids as well as reactions with H_2SO_4 and HNO_3 to create organosulfate and organonitrates or respond with ammonia to form reduced-nitrogen-containing compounds (Liu et al., 2015) (Ervens et al., 2011).

3.3 Evolution of CHON compounds and functionality

CHON compounds were the most abundant group in the (+)ESI results, accounting for 79 %–83 % in number frequency. The average molecular weight decreased during the daytime, from 418 Da in MEM to 402 in the morning and 399 in the afternoon and then increased to 405 at night. O/C_w varied from 0.13 to 0.14, while H/C_w was between 1.74 to 1.82. O/C_w was lower than 0.18, and H/C_w was higher than 1.5 (Table 1). The HMWOCs in the range of the above parameters were likely from biomass burning, as reported in a previous study by Song et al., 2022.

As shown in Fig. 5, most CHON compounds, accounting for 60 %–63 %, had $H : C_w > 1.7$ and AI < 0.15. These CHON compounds were nitrogen-containing, and most had –NO2 or –ONO2, namely unsaturated organonitrate. The details of CHON compounds with higher O/N ratios (≥ 3) are discussed in the following text. The unsaturated organonitrates were more pronounced in both MEM and the afternoon, making up up to 63.2 % and 63.3 %, respectively. The highly unsaturated organonitrates ($H : C = 0.7$–1.5 and $0.15 < AI < 0.5$) decreased from 33.8 % in the morning to 21.6 % in the afternoon, possibly due to the influence of photobleaching from daytime photochemical activities (Q. He et al., 2021). Also, the aromatic CHON (AI > 0.5) increased to 3.1 % at night.

The diagram of OS_c against carbon number is shown in Fig. 6. Most CHON compounds are distributed in a range of carbon numbers between 10 and 40 and OS_c between −2 and 1. The long-chain nitro-hydrocarbon with carbon numbers between 30 and 60 were substantially enhanced by the morning rush hours. During the daytime, CHON compounds with carbon numbers between 10 and 30 and OS_c between −1 and 0 were enhanced, suggesting that more aged nitro-hydrocarbons were produced in the daytime.

Typically, CHON compounds with higher O/N ratios (≥ 3) can be attributed to organic nitrate ($RONO_2$) groups in +ESI mode (Song et al., 2022). The organonitrates accounted for 21.9 %–24.0 % of CHON compounds, and the associated ratios of log RI were between 22.2 %–23.0 %. $RONO_2$ compounds were more prominent in the morning (24.0 %) and lower without sunlight (e.g., 21.9 % in MEM). $RONO_2$ compounds with AI > 0.5, attributed to polycyclic phenolic compounds, increased in the morning (from 1.7 % to 2.1 % after the rush hour), then decreased to 1.9 % in the afternoon, and then increased to 2.0 % at night.

As shown in Fig. S6, N_1O_x ($x = 1$–9) with DBE < 5 was the most abundant in the CHON subgroup, accounting for 49 %–51 % of CHON compounds in number frequency. Since most CHON compounds contained only one nitrogen atom, the $CHON_1$ group was chosen for further evaluation. Figure 7 shows that the $CHON_1$ CH_2 homologues with a molecular mass between 150 and 400 were stable and resistant, as shown in Fig. 7a–c. However, $CHON_1$ compounds with M.W. smaller than 200 were removed in the afternoon but produced at night. The nighttime chemistry strongly removed the $CHON_1$ CH_2 homologues with M.W. > 600 (Fig. 7c). These results suggest the diversities of the atmospheric fate of $CHON_1$ compounds.

From the point of view of KMD, as shown in Fig. 7d–f, $CHON_1$ compounds (COO homologous) were removed in the morning, while they were produced prominently in the afternoon and at night (Fig. 7d and e). These results suggest that the organonitrates continued performing multi-generation oxidation to produce more carboxylic functional

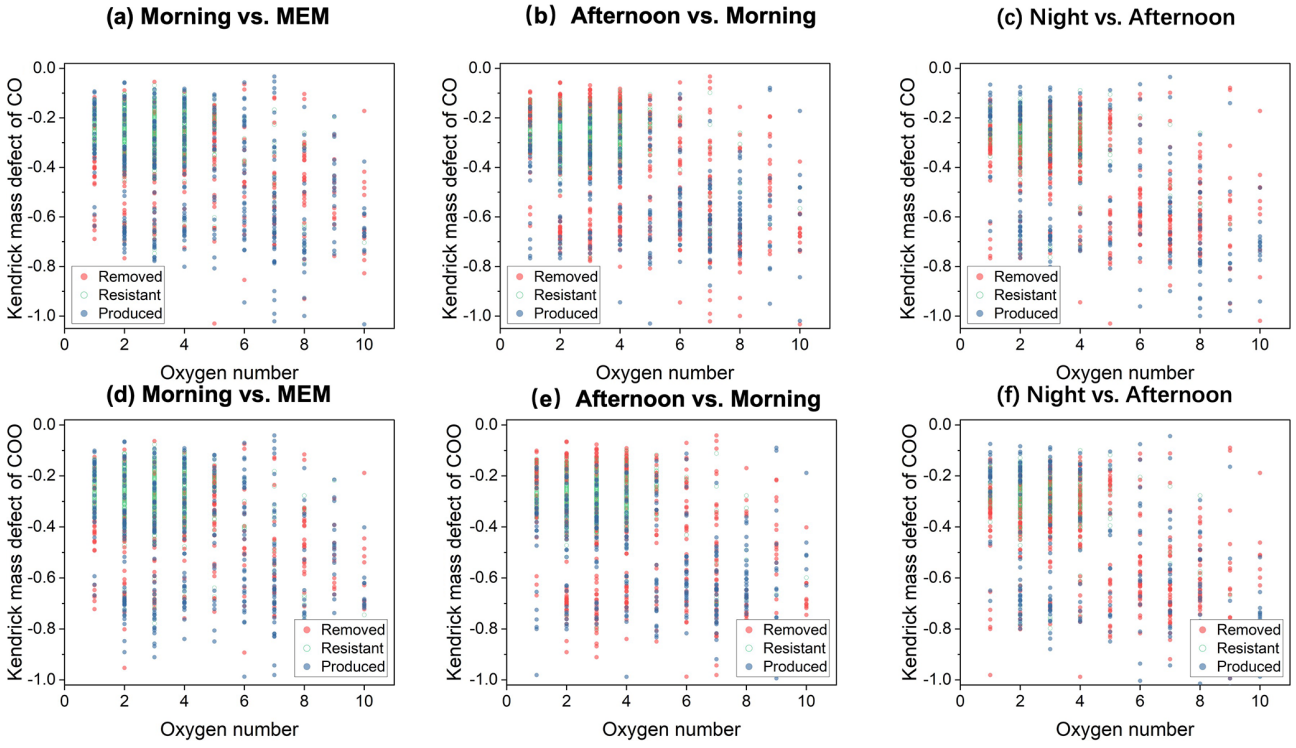

Figure 4. Kendrick mass defect (KMD) plots of CHO compounds in the diurnal evolution of CO series **(a–c)** and COO series **(d–f)**.

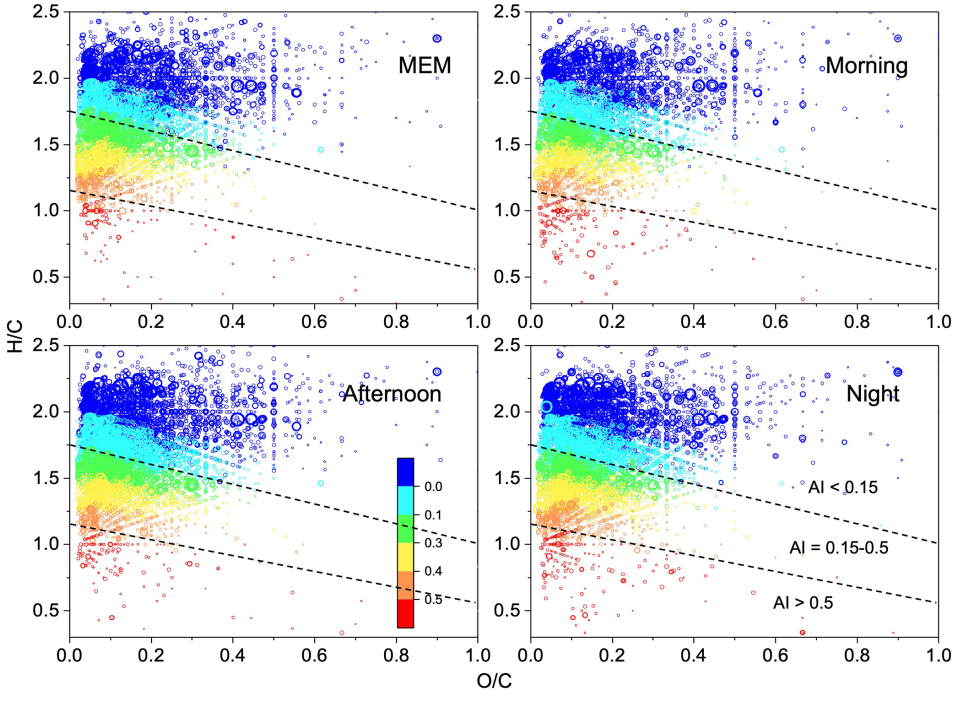

Figure 5. Van Krevelen diagrams (H/C vs. O/C ratio) for CHON species with various aromatic index (AI) value ranges. The dashed lines separate the different AI regions, and the color bar is AI values.

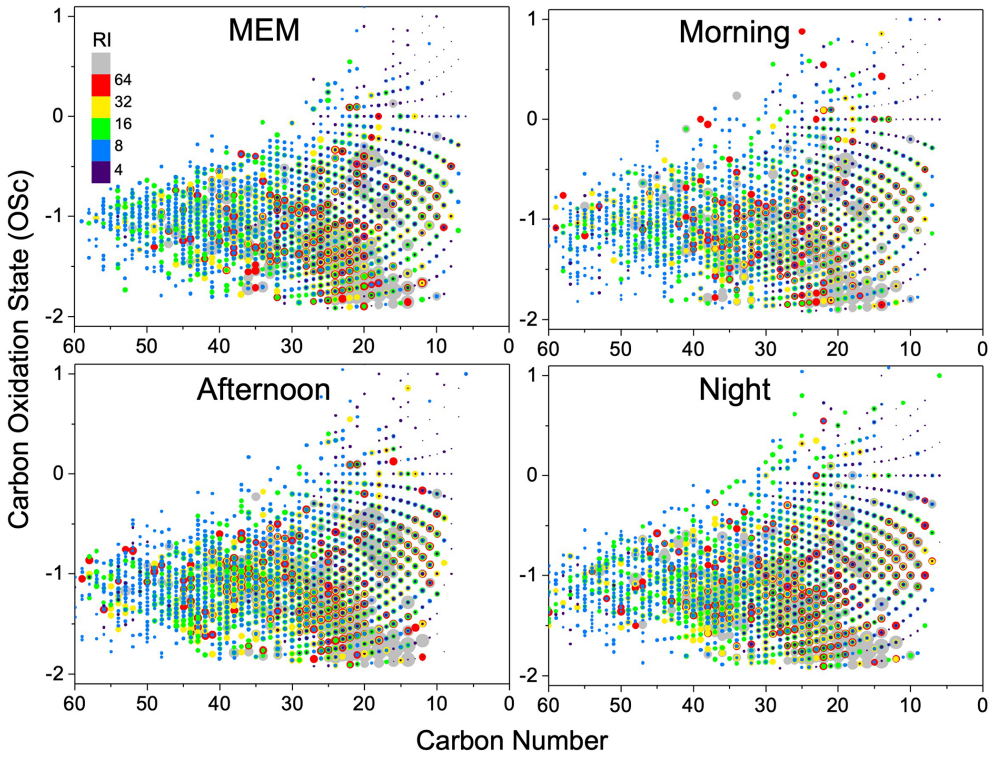

Figure 6. Overlaid carbon oxidation state (OS_c) symbols for CHON species. The size and color bar of the markers reflects the relative peak intensities of molecular formulae on a logarithmic scale. RI: relative intensity.

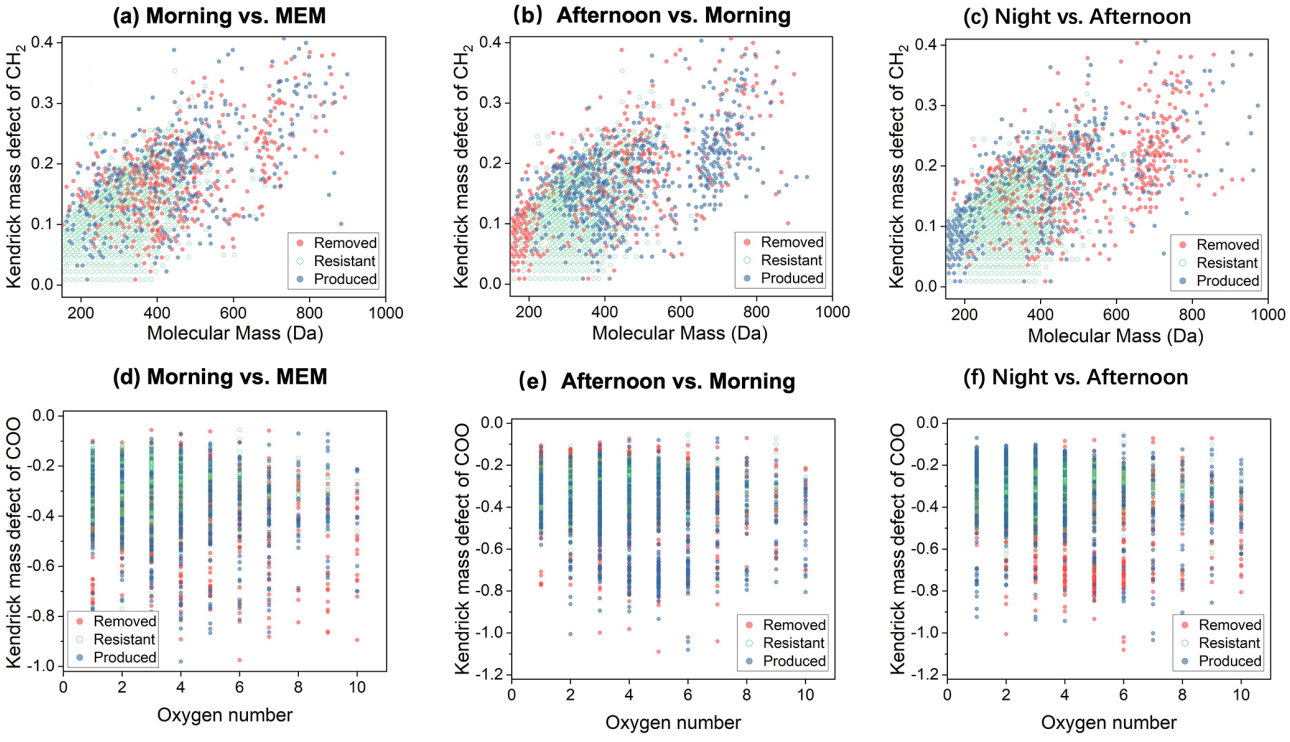

Figure 7. Kendrick mass defect (KMD) plots of $CHON_1$ compounds in the diurnal evolution of CH_2 series **(a–c)** and COO series **(d–f)**.

groups (–COOH), and the carboxylic functional groups may be due to the reaction with acids such as HNO_3 and H_2SO_4, forming organonitrate and organosulfates or being neutralized by NH_3 to form ammonium salt or reduced N-containing compounds in the particle phase (Lim et al., 2016; Darer et al., 2011; Zarzana et al., 2012). In previous studies, these processes were proven to occur in small carboxylic acids. In this work, we can observe a similar process in HMWOCs.

3.4 CHN compounds' evolution and functionality

CHN compounds remained stable in the FT-ICR MS dataset, accounting for 9 %–10 % in number and 3 %–10 % in intensity. The average H/C_w was between 1.30 and 1.51 among four samples. As shown in the DBE against carbon number diagram (Fig. 8), most CHN compounds have carbon numbers between 10 and 60 as well as nitrogen numbers from 1 to 10. Only a trivial proportion (3.0 %–4.5 %) of CHN compounds has a DBE = 0 and carbon numbers > 10 as long-chain aliphatic amines (Song et al., 2022). Long-chain aliphatic amines could be emitted from traffic and biomass emissions in the morning, then decrease to 3.0 % in the afternoon, and finally reach 4.5 % at night due to rising relative humidity (Chen et al., 2019).

CHN compounds with two nitrogen atoms (N_2) and DBE > 5 were the most abundant group. For example, the series of $C_5H_8N_2(CH_2)_n$, $C_5H_6N_2(CH_2)_n$, and $C_7H_6N_2(CH_2)_n$ homologous series were likely imidazole, pyrazine/pyrimidine, and azaindole homologous series, respectively (Wang et al., 2019). In total, 16 %–18 % of N_2-containing CHN compounds were attributed to five-membered rings such as pyrazole, imidazole, and their derivatives, or six-membered rings, such as N-heterocyclic species. The abundance of N_2-containing CHN compounds showed an increasing trend from 16.3 % (MEM) to 27.2 % at night.

CHN compounds with a nitrogen number(N_n) greater than eight occurred in both day- and nighttime, suggesting the impact of the secondary formation of CHN compounds. After diurnal processing, the relative intensities of CHN compounds, with C numbers between 20 and 50, were enhanced (Fig. 8). This result was consistent with the KMD analysis, as shown in Fig. 9.

The $N_{8–10}$-containing CHN compounds accounted for 11.4 %–18.5 % among the four stages, appearing with homologous series. They typically appeared with carbon numbers larger than 20, with the largest abundance in MEM (18.5 %). These CHN compounds can be vaporized from coal burning, especially in the smoldering stages. Therefore, the $N_{8–10}$-containing CHN compounds were reasonably more pronounced at low temperatures from residential coal use for heating. Besides the primary emission, small CHN compounds can also form from the reactions between amines and ammonia and carbonyl-containing SOA (Zarzana et al., 2012; Liu et al., 2015). Our results suggested that the formation of HMW CHN was also possible.

4 Atmospheric implications

It is noticeable that there were some limitations on this work. Under variable emissions, atmospheric processs, and long-distance transport of organic aerosols, the samples can give a snapshot the evolution in the region, and the analysis can cause uncertainties. Therefore, this work can be treated as a case study. This study is an attempt to evaluate the evolution of high molecular-weight organics using FT-ICR MS. Since the technique is a non-quantitative and the matrix effect cannot be ignored, these facts lead to considerable uncertainties. When discussing the evolution of HMWOCs, it is noticeable that the formation of higher oxidative groups, such as carbonyl or carboxylic acid groups, were commonly accompanied by the loss of other atoms such as hydrogen or even the breaking-up of the carbon chain. However, those process are difficult to illustrate using the FT-ICR MS method.

We present the molecular description of the diurnal evolution of HMWOCs that is sensitive to the (+)ESI mode in FT-ICR MS analysis to explore the wider context of HMWOCs. The uptake of ammonia on biogenic or anthropogenic SOA to form light-absorbing nitrogen-containing organics has been reported (K. Li et al., 2017; Liu et al., 2015). In this study, we proved that the nucleophilic oxygenated and nitrogen-containing compounds can also undergo substantial aging. Commonly, the nucleophilic HMWOCs were considered less polar, and their evolution was different. We found more –CHO and –COOH groups were detected in the daytime for the CHO subgroup, and the aerosol-phase oxidation continued in the dark, resulting in more oxidized HMWOCs.

The formation of HMW organonitrates was also complicated. We have observed the prominence of organonitrates in both the day and at night. In the daytime, the possible pathway includes the reactions of NO_2 radicals with aliphatic hydrocarbons and aromatic rings. At nighttime, the adduct of the NO_3 radical on HMWOCs could possibly occur. In polluted urban areas, the rich nitrogen oxide (NO_x) environment produced nitrate as well as organonitrates. The processing can shift the nitrogen deposition and be important on a local or regional scale. Also, the $CHON_1$ compounds occurred along with carboxylation, suggesting that the multiple oxidations of organonitrates can occur in both the day- and nighttime. The process can enhance hygroscopic growth and cloud condensation nuclei (CCN) activities due to the acid–base reactions between ammonia and organics with carboxylic acids (Dinar et al., 2008).

The daytime CHN compounds could be produced from the condensation reaction between –CHO groups and ammonium/amines. This might indicate that the formation of long-chain CHN might be less important; however, these species have possibly five- or six-member rings that can act as chro-

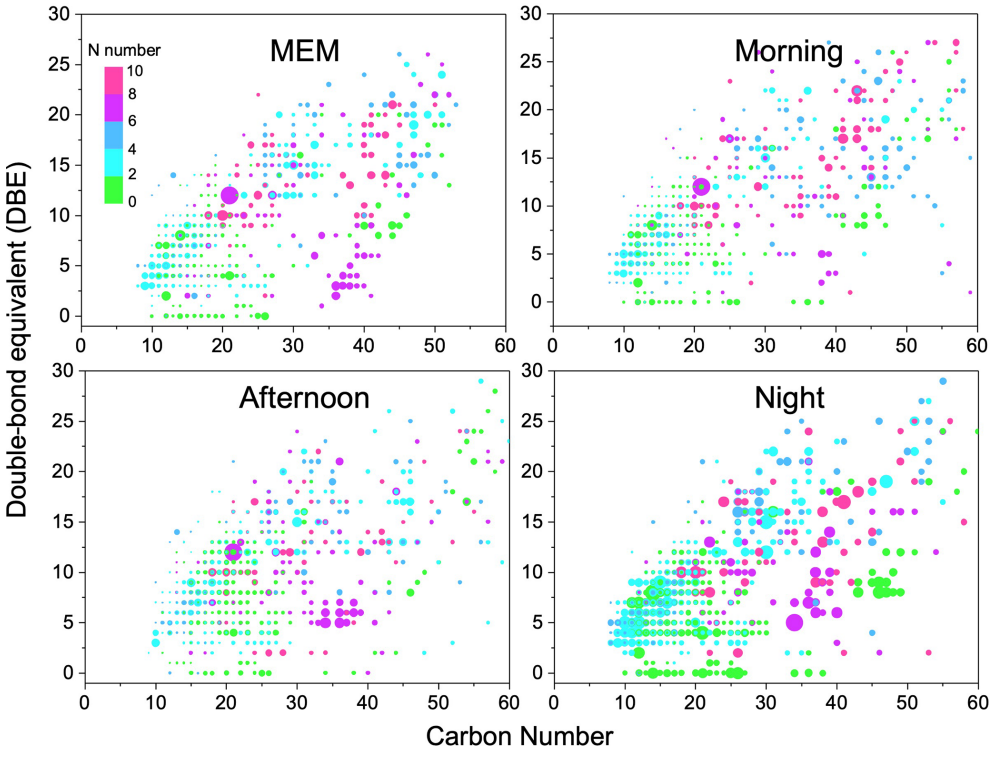

Figure 8. Carbon number vs. double-bond equivalent (DBE) for CHN species. The color bar denotes the number of N atoms. The size of the symbols reflects the relative peak intensities of molecular formulae on a logarithmic scale.

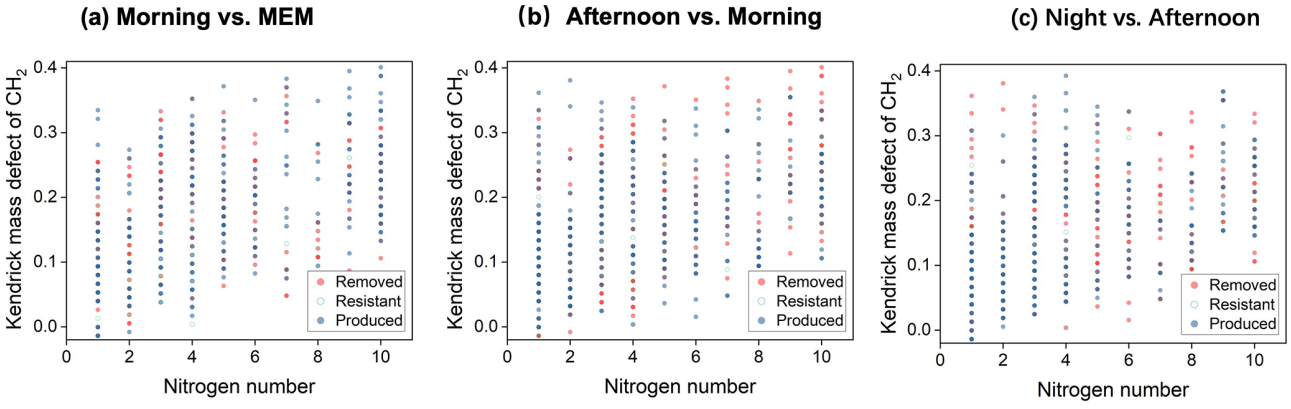

Figure 9. Kendrick mass defect (KMD) plots of CHN compounds in the diurnal evolution of CH_2 series **(a–c)**.

mophores. Along with the primary emission of HMW CHN from coal combustion and biomass burning (Brege et al., 2018; Ray et al., 2019), the sources of BrC should be reconsidered. Moreover, the impact of ammonia was commonly considered with regard to its potential impact on nitrogen deposition or forming the secondary organic aerosol, but we suggest assessing its effect on the formation of HMW BrC. In conclusion, the evaluation of nucleophilic HMWOC properties due to variability should be considered in future studies for an improvement in air quality and climate model performances.

Data availability. Data supporting this paper can be found at https://doi.org/10.5281/zenodo.7830299 (Chen, 2023).

Supplement. The supplement related to this article is available online at: https://doi.org/10.5194/acp-24-1627-2024-supplement.

Author contributions. YC designed this study. QL, CH, MH, and HChe contributed to the data collected during the field campaign. JZ, SZ, and YX performed field experiments. CH did data analysis and drafting; HC, ZB, YL, QL, MH, JZ, and SZ did sample collec-

tion and methodology; XY, QS, CC, YH, LM, XL, and FY carried scientific discussion; YC was responsible for funding acquisition, resources, and writing (review and editing).

Competing interests. The contact author has declared that none of the authors has any competing interests.

Disclaimer. Publisher's note: Copernicus Publications remains neutral with regard to jurisdictional claims made in the text, published maps, institutional affiliations, or any other geographical representation in this paper. While Copernicus Publications makes every effort to include appropriate place names, the final responsibility lies with the authors.

Acknowledgements. The authors are grateful for the assistance of colleagues for sample collection.

Financial support. This research has been supported by the National Natural Science Foundation of China (grant nos. 42003059, 42075109, and 42107452) and the Science Foundation of China University of Petroleum, Beijing (grant no. 2462023YJRC003).

Review statement. This paper was edited by Jason Surratt and reviewed by two anonymous referees.

References

Antony, R., Grannas, A. M., Willoughby, A. S., Sleighter, R. L., Thamban, M., and Hatcher, P. G.: Origin and sources of dissolved organic matter in snow on the East Antarctic ice sheet, Environ. Sci. Technol., 48, 6151–6159, https://doi.org/10.1021/es405246a, 2014.

Ao, M., Pham, G. H., Sunarso, J., Tade, M. O., and Liu, S.: Active centers of catalysts for higher alcohol synthesis from syngas: a review, ACS Catal., 8, 7025–7050, 2018.

Bandowe, B. A. M. and Meusel, H.: Nitrated polycyclic aromatic hydrocarbons (nitro-PAHs) in the environment – A review, Sci. Total. Environ., 581–582, 237–257, https://doi.org/10.1016/j.scitotenv.2016.12.115, 2017.

Bianco, A., Deguillaume, L., Vaitilingom, M., Nicol, E., Baray, J. L., Chaumerliac, N., and Bridoux, M.: Molecular Characterization of Cloud Water Samples Collected at the Puy de Dome (France) by Fourier Transform Ion Cyclotron Resonance Mass Spectrometry, Environ. Sci. Technol., 52, 10275–10285, https://doi.org/10.1021/acs.est.8b01964, 2018.

Brege, M., Paglione, M., Gilardoni, S., Decesari, S., Facchini, M. C., and Mazzoleni, L. R.: Molecular insights on aging and aqueous-phase processing from ambient biomass burning emissions-influenced Po Valley fog and aerosol, Atmos. Chem. Phys., 18, 13197–13214, https://doi.org/10.5194/acp-18-13197-2018, 2018.

Chen, Y.: Diurnal Evolution of Nucleophilic High-molecular-weight Organic Compounds in Ambient Aerosols, Zenodo [data set], https://doi.org/10.5281/zenodo.7830299, 2023.

Chen, Y., Cao, J., Zhao, J., Xu, H., Arimoto, R., Wang, G., Han, Y., Shen, Z., and Li, G.: N-alkanes and polycyclic aromatic hydrocarbons in total suspended particulates from the southeastern Tibetan Plateau: concentrations, seasonal variations, and sources, Sci. Total. Environ., 470–471, 9–18, https://doi.org/10.1016/j.scitotenv.2013.09.033, 2014.

Chen, Y., Tian, M., Huang, R.-J., Shi, G., Wang, H., Peng, C., Cao, J., Wang, Q., Zhang, S., Guo, D., Zhang, L., and Yang, F.: Characterization of urban amine-containing particles in southwestern China: seasonal variation, source, and processing, Atmos. Chem. Phys., 19, 3245–3255, https://doi.org/10.5194/acp-19-3245-2019, 2019.

Creamean, J. M., Lee, C., Hill, T. C., Ault, A. P., DeMott, P. J., White, A. B., Ralph, F. M., and Prather, K. A.: Chemical properties of insoluble precipitation residue particles, J. Aerosol Sci., 76, 13–27, https://doi.org/10.1016/j.jaerosci.2014.05.005, 2014.

Darer, A. I., Cole-Filipiak, N. C., O'Connor, A. E., and Elrod, M. J.: Formation and stability of atmospherically relevant isoprene-derived organosulfates and organonitrates, Environ. Sci. Technol., 45, 1895–1902, 2011.

Dinar, E., Anttila, T., and Rudich, Y.: CCN activity and hygroscopic growth of organic aerosols following reactive uptake of ammonia, Environ. Sci. Technol., 42, 793–799, 2008.

Ditto, J. C., Barnes, E. B., Khare, P., Takeuchi, M., Joo, T., Bui, A. A. T., Lee-Taylor, J., Eris, G., Chen, Y., Aumont, B., Jimenez, J. L., Ng, N. L., Griffin, R. J., and Gentner, D. R.: An omnipresent diversity and variability in the chemical composition of atmospheric functionalized organic aerosol, Communications Chemistry, 1, 75, https://doi.org/10.1038/s42004-018-0074-3, 2018.

Ditto, J. C., He, M., Hass-Mitchell, T. N., Moussa, S. G., Hayden, K., Li, S.-M., Liggio, J., Leithead, A., Lee, P., Wheeler, M. J., Wentzell, J. J. B., and Gentner, D. R.: Atmospheric evolution of emissions from a boreal forest fire: the formation of highly functionalized oxygen-, nitrogen-, and sulfur-containing organic compounds, Atmos. Chem. Phys., 21, 255–267, https://doi.org/10.5194/acp-21-255-2021, 2021.

Ervens, B., Turpin, B. J., and Weber, R. J.: Secondary organic aerosol formation in cloud droplets and aqueous particles (aqSOA): a review of laboratory, field and model studies, Atmos. Chem. Phys., 11, 11069–11102, https://doi.org/10.5194/acp-11-11069-2011, 2011.

George, C., Ammann, M., D'Anna, B., Donaldson, D. J., and Nizkorodov, S. A.: Heterogeneous photochemistry in the atmosphere, Chem. Rev., 115, 4218–4258, https://doi.org/10.1021/cr500648z, 2015.

Hallquist, M., Wenger, J. C., Baltensperger, U., Rudich, Y., Simpson, D., Claeys, M., Dommen, J., Donahue, N. M., George, C., Goldstein, A. H., Hamilton, J. F., Herrmann, H., Hoffmann, T., Iinuma, Y., Jang, M., Jenkin, M. E., Jimenez, J. L., Kiendler-Scharr, A., Maenhaut, W., McFiggans, G., Mentel, Th. F., Monod, A., Prévôt, A. S. H., Seinfeld, J. H., Surratt, J. D., Szmigielski, R., and Wildt, J.: The formation, properties and impact of secondary organic aerosol: current and emerging issues, Atmos. Chem. Phys., 9, 5155–5236, https://doi.org/10.5194/acp-9-5155-2009, 2009.

He, C., Fang, Z., Li, Y., Jiang, C., Zhao, S., Xu, C., Zhang, Y., and Shi, Q.: Ionization selectivity of electrospray and atmospheric pressure photoionization FT-ICR MS for petroleum refinery wastewater dissolved organic matter, Environ. Sci.-Proc. Imp., 23, 1466–1475, https://doi.org/10.1039/d1em00248a, 2021.

He, C., He, D., Chen, C., and Shi, Q.: Application of Fourier Transform Ion Cyclotron Resonance Mass Spectrometry in molecular characterization of dissolved organic matter, Sci. China Earth Sci., 65, 2219–2236, https://doi.org/10.1360/SSTe-2021-0390, 2022.

He, Q., Tomaz, S., Li, C., Zhu, M., Meidan, D., Riva, M., Laskin, A., Brown, S. S., George, C., Wang, X., and Rudich, Y.: Optical Properties of Secondary Organic Aerosol Produced by Nitrate Radical Oxidation of Biogenic Volatile Organic Compounds, Environ. Sci. Technol., 55, 2878–2889, https://doi.org/10.1021/acs.est.0c06838, 2021.

Hodshire, A. L., Akherati, A., Alvarado, M. J., Brown-Steiner, B., Jathar, S. H., Jimenez, J. L., Kreidenweis, S. M., Lonsdale, C. R., Onasch, T. B., Ortega, A. M., and Pierce, J. R.: Aging Effects on Biomass Burning Aerosol Mass and Composition: A Critical Review of Field and Laboratory Studies, Environ. Sci. Technol., 53, 10007–10022, https://doi.org/10.1021/acs.est.9b02588, 2019.

Huang, R. J., Zhang, Y., Bozzetti, C., Ho, K. F., Cao, J. J., Han, Y., Daellenbach, K. R., Slowik, J. G., Platt, S. M., Canonaco, F., Zotter, P., Wolf, R., Pieber, S. M., Bruns, E. A., Crippa, M., Ciarelli, G., Piazzalunga, A., Schwikowski, M., Abbaszade, G., Schnelle-Kreis, J., Zimmermann, R., An, Z., Szidat, S., Baltensperger, U., El Haddad, I., and Prevot, A. S.: High secondary aerosol contribution to particulate pollution during haze events in China, Nature, 514, 218–222, https://doi.org/10.1038/nature13774, 2014.

Jiang, B., Liang, Y., Xu, C., Zhang, J., Hu, M., and Shi, Q.: Polycyclic aromatic hydrocarbons (PAHs) in ambient aerosols from Beijing: characterization of low volatile PAHs by positive-ion atmospheric pressure photoionization (APPI) coupled with Fourier transform ion cyclotron resonance, Environ. Sci. Technol., 48, 4716–4723, https://doi.org/10.1021/es405295p, 2014.

Jimenez, J. L., Canagaratna, M. R., Donahue, N. M., Prevot, A. S., Zhang, Q., Kroll, J. H., DeCarlo, P. F., Allan, J. D., Coe, H., Ng, N. L., Aiken, A. C., Docherty, K. S., Ulbrich, I. M., Grieshop, A. P., Robinson, A. L., Duplissy, J., Smith, J. D., Wilson, K. R., Lanz, V. A., Hueglin, C., Sun, Y. L., Tian, J., Laaksonen, A., Raatikainen, T., Rautiainen, J., Vaattovaara, P., Ehn, M., Kulmala, M., Tomlinson, J. M., Collins, D. R., Cubison, M. J., Dunlea, E. J., Huffman, J. A., Onasch, T. B., Alfarra, M. R., Williams, P. I., Bower, K., Kondo, Y., Schneider, J., Drewnick, F., Borrmann, S., Weimer, S., Demerjian, K., Salcedo, D., Cottrell, L., Griffin, R., Takami, A., Miyoshi, T., Hatakeyama, S., Shimono, A., Sun, J. Y., Zhang, Y. M., Dzepina, K., Kimmel, J. R., Sueper, D., Jayne, J. T., Herndon, S. C., Trimborn, A. M., Williams, L. R., Wood, E. C., Middlebrook, A. M., Kolb, C. E., Baltensperger, U., and Worsnop, D. R.: Evolution of organic aerosols in the atmosphere, Science, 326, 1525–1529, https://doi.org/10.1126/science.1180353, 2009.

Kanawati, B., Herrmann, F., Joniec, S., Winterhalter, R., and Moortgat, G. K.: Mass spectrometric characterization of beta-caryophyllene ozonolysis products in the aerosol studied using an electrospray triple quadrupole and time-of-flight analyzer hybrid system and density functional theory, Rapid Commun. Mass Sp., 22, 165–186, https://doi.org/10.1002/rcm.3340, 2008.

Koch, B. P. and Dittmar, T.: From mass to structure: an aromaticity index for high-resolution mass data of natural organic matter, Rapid Commun. Mass Sp., 20, 926–932, https://doi.org/10.1002/rcm.2386, 2006.

Kroll, J. H., Donahue, N. M., Jimenez, J. L., Kessler, S. H., Canagaratna, M. R., Wilson, K. R., Altieri, K. E., Mazzoleni, L. R., Wozniak, A. S., Bluhm, H., Mysak, E. R., Smith, J. D., Kolb, C. E., and Worsnop, D. R.: Carbon oxidation state as a metric for describing the chemistry of atmospheric organic aerosol, Nat. Chem., 3, 133–139, https://doi.org/10.1038/nchem.948, 2011.

Kurek, M. R., Poulin, B. A., McKenna, A. M., and Spencer, R. G. M.: Deciphering Dissolved Organic Matter: Ionization, Dopant, and Fragmentation Insights via Fourier Transform-Ion Cyclotron Resonance Mass Spectrometry, Environ. Sci. Technol., 54, 16249–16259, https://doi.org/10.1021/acs.est.0c05206, 2020.

Laskin, J., Laskin, A., Nizkorodov, S. A., Roach, P., Eckert, P., Gilles, M. K., Wang, B., Lee, H. J., and Hu, Q.: Molecular selectivity of brown carbon chromophores, Environ. Sci. Technol., 48, 12047–12055, https://doi.org/10.1021/es503432r, 2014.

Li, H., Zhang, Q., Zhang, Q., Chen, C., Wang, L., Wei, Z., Zhou, S., Parworth, C., Zheng, B., Canonaco, F., Prévôt, A. S. H., Chen, P., Zhang, H., Wallington, T. J., and He, K.: Wintertime aerosol chemistry and haze evolution in an extremely polluted city of the North China Plain: significant contribution from coal and biomass combustion, Atmos. Chem. Phys., 17, 4751–4768, https://doi.org/10.5194/acp-17-4751-2017, 2017.

Li, K., Li, J., Liggio, J., Wang, W., Ge, M., Liu, Q., Guo, Y., Tong, S., Li, J., Peng, C., Jing, B., Wang, D., and Fu, P.: Enhanced Light Scattering of Secondary Organic Aerosols by Multiphase Reactions, Environ. Sci. Technol., 51, 1285–1292, https://doi.org/10.1021/acs.est.6b03229, 2017.

Li, X., Yu, F., Cao, J., Fu, P., Hua, X., Chen, Q., Li, J., Guan, D., Tripathee, L., Chen, Q., and Wang, Y.: Chromophoric dissolved organic carbon cycle and its molecular compositions and optical properties in precipitation in the Guanzhong basin, China, Sci. Total. Environ., 814, 152775, https://doi.org/10.1016/j.scitotenv.2021.152775, 2022.

Liggio, J. and Li, S.-M.: Organosulfate formation during the uptake of pinonaldehyde on acidic sulfate aerosols, Geophys. Res. Lett., 33, L13808-L13808, https://doi.org/10.1029/2006gl026079, 2006.

Lim, Y. B., Kim, H., Kim, J. Y., and Turpin, B. J.: Photochemical organonitrate formation in wet aerosols, Atmos. Chem. Phys., 16, 12631–12647, https://doi.org/10.5194/acp-16-12631-2016, 2016.

Lin, P., Rincon, A. G., Kalberer, M., and Yu, J. Z.: Elemental composition of HULIS in the Pearl River Delta Region, China: results inferred from positive and negative electrospray high resolution mass spectrometric data, Environ. Sci. Technol., 46, 7454–7462, https://doi.org/10.1021/es300285d, 2012.

Liu, Y., Liggio, J., Staebler, R., and Li, S.-M.: Reactive uptake of ammonia to secondary organic aerosols: kinetics of organonitrogen formation, Atmos. Chem. Phys., 15, 13569–13584, https://doi.org/10.5194/acp-15-13569-2015, 2015.

McGuire, M. L., Chang, R. Y.-W., Slowik, J. G., Jeong, C.-H., Healy, R. M., Lu, G., Mihele, C., Abbatt, J. P. D., Brook, J. R., and Evans, G. J.: Enhancing non-refractory aerosol apportionment from an urban industrial site through receptor model-

ing of complete high time-resolution aerosol mass spectra, Atmos. Chem. Phys., 14, 8017–8042, https://doi.org/10.5194/acp-14-8017-2014, 2014.

Pöschl, U.: Atmospheric Aerosols: Composition, Transformation, Climate and Health Effects, Angew. Chem. Int. Ed., 44, 7520–7540, https://doi.org/10.1002/anie.200501122, 2005.

Ray, D., Singh, S., Ghosh, S. K., and Raha, S.: Dynamic response of light absorption by $PM_{2.5}$ bound water-soluble organic carbon to heterogeneous oxidation, Aerosol Sci. Technol., 53, 1404–1414, https://doi.org/10.1080/02786826.2019.1661350, 2019.

Rice, S., Maurer, D. L., Fennell, A., Dharmadhikari, M., and Koziel, J. A.: Evaluation of Volatile Metabolites Emitted In-Vivo from Cold-Hardy Grapes during Ripening Using SPME and GC-MS: A Proof-of-Concept, Molecules, 24, 536, https://doi.org/10.3390/molecules24030536, 2019.

Seidel, M., Beck, M., Riedel, T., Waska, H., Suryaputra, I. G. N. A., Schnetger, B., Niggemann, J., Simon, M., and Dittmar, T.: Biogeochemistry of dissolved organic matter in an anoxic intertidal creek bank, Geochim. Cosmochim. Ac., 140, 418–434, https://doi.org/10.1016/j.gca.2014.05.038, 2014.

Song, J., Li, M., Zou, C., Cao, T., Fan, X., Jiang, B., Yu, Z., Jia, W., and Peng, P.: Molecular Characterization of Nitrogen-Containing Compounds in Humic-like Substances Emitted from Biomass Burning and Coal Combustion, Environ. Sci. Technol., 56, 119–130, https://doi.org/10.1021/acs.est.1c04451, 2022.

Stenson, A. C., Marshall, A. G., and Cooper, W. T.: Exact masses and chemical formulas of individual Suwannee River fulvic acids from ultrahigh resolution electrospray ionization Fourier transform ion cyclotron resonance mass spectra, Anal. Chem., 75, 1275–1284, https://doi.org/10.1021/ac026106p, 2003.

Tang, J., Li, J., Su, T., Han, Y., Mo, Y., Jiang, H., Cui, M., Jiang, B., Chen, Y., Tang, J., Song, J., Peng, P., and Zhang, G.: Molecular compositions and optical properties of dissolved brown carbon in biomass burning, coal combustion, and vehicle emission aerosols illuminated by excitation–emission matrix spectroscopy and Fourier transform ion cyclotron resonance mass spectrometry analysis, Atmos. Chem. Phys., 20, 2513–2532, https://doi.org/10.5194/acp-20-2513-2020, 2020.

Tao, J., Zhang, L., Cao, J., and Zhang, R.: A review of current knowledge concerning $PM_{2.5}$ chemical composition, aerosol optical properties and their relationships across China, Atmos. Chem. Phys., 17, 9485–9518, https://doi.org/10.5194/acp-17-9485-2017, 2017.

Wang, H., Qiao, B., Zhang, L., Yang, F., and Jiang, X.: Characteristics and sources of trace elements in $PM_{2.5}$ in two megacities in Sichuan Basin of southwest China, Environ. Pollut., 242, 1577–1586, https://doi.org/10.1016/j.envpol.2018.07.125, 2018.

Wang, Y., Hu, M., Lin, P., Tan, T., Li, M., Xu, N., Zheng, J., Du, Z., Qin, Y., Wu, Y., Lu, S., Song, Y., Wu, Z., Guo, S., Zeng, L., Huang, X., and He, L.: Enhancement in Particulate Organic Nitrogen and Light Absorption of Humic-Like Substances over Tibetan Plateau Due to Long-Range Transported Biomass Burning Emissions, Environ. Sci. Technol., 53, 14222–14232, https://doi.org/10.1021/acs.est.9b06152, 2019.

Xie, Q., Su, S., Chen, S., Xu, Y., Cao, D., Chen, J., Ren, L., Yue, S., Zhao, W., Sun, Y., Wang, Z., Tong, H., Su, H., Cheng, Y., Kawamura, K., Jiang, G., Liu, C.-Q., and Fu, P.: Molecular characterization of firework-related urban aerosols using Fourier transform ion cyclotron resonance mass spectrometry, Atmos. Chem. Phys., 20, 6803–6820, https://doi.org/10.5194/acp-20-6803-2020, 2020.

Yu, L., Smith, J., Laskin, A., George, K. M., Anastasio, C., Laskin, J., Dillner, A. M., and Zhang, Q.: Molecular transformations of phenolic SOA during photochemical aging in the aqueous phase: competition among oligomerization, functionalization, and fragmentation, Atmos. Chem. Phys., 16, 4511–4527, https://doi.org/10.5194/acp-16-4511-2016, 2016.

Yun, Y., Liang, L., Wei, Y., Luo, Z., Yuan, F., Li, G., and Sang, N.: Exposure to Nitro-PAHs interfere with germination and early growth of Hordeum vulgare via oxidative stress, Ecotox. Environ. Safe., 180, 756–761, https://doi.org/10.1016/j.ecoenv.2019.05.032, 2019.

Zarzana, K. J., De Haan, D. O., Freedman, M. A., Hasenkopf, C. A., and Tolbert, M. A.: Optical Properties of the Products of α-Dicarbonyl and Amine Reactions in Simulated Cloud Droplets, Environ. Sci. Technol., 46, 4845–4851, https://doi.org/10.1021/es2040152, 2012.

Zhang, Q., Jimenez, J. L., Canagaratna, M. R., Allan, J. D., Coe, H., Ulbrich, I., Alfarra, M. R., Takami, A., Middlebrook, A. M., Sun, Y. L., Dzepina, K., Dunlea, E., Docherty, K., DeCarlo, P. F., Salcedo, D., Onasch, T., Jayne, J. T., Miyoshi, T., Shimono, A., Hatakeyama, S., Takegawa, N., Kondo, Y., Schneider, J., Drewnick, F., Borrmann, S., Weimer, S., Demerjian, K., Williams, P., Bower, K., Bahreini, R., Cottrell, L., Griffin, R. J., Rautiainen, J., Sun, J. Y., Zhang, Y. M., and Worsnop, D. R.: Ubiquity and dominance of oxygenated species in organic aerosols in anthropogenically-influenced Northern Hemisphere midlatitudes, Geophys. Res. Lett., 34, L13801, https://doi.org/10.1029/2007gl029979, 2007.

Zhang, Q., Jimenez, J. L., Canagaratna, M. R., Ulbrich, I. M., Ng, N. L., Worsnop, D. R., and Sun, Y.: Understanding atmospheric organic aerosols via factor analysis of aerosol mass spectrometry: a review, Anal. Bioanal. Chem., 401, 3045–3067, https://doi.org/10.1007/s00216-011-5355-y, 2011.

Zhang, R., Wang, G., Guo, S., Zamora, M. L., Ying, Q., Lin, Y., Wang, W., Hu, M., and Wang, Y.: Formation of urban fine particulate matter, Chem. Rev., 115, 3803–3855, https://doi.org/10.1021/acs.chemrev.5b00067, 2015.

Zhang, Z., Zhao, W., Hu, W., Deng, J., Ren, L., Wu, L., Chen, S., Meng, J., Pavuluri, C. M., Sun, Y., Wang, Z., Kawamura, K., and Fu, P.: Molecular characterization and spatial distribution of dicarboxylic acids and related compounds in fresh snow in China, Environ. Pollut., 291, 118114, https://doi.org/10.1016/j.envpol.2021.118114, 2021.